THE UNIVERSITY of WISCONSIN MADISON

Influence of HSX Geometry on Drift Waves

Tariq Rafiq and C.C. Hegna

US/Japan meeting 2006

THE UNIVERSITY of WISCONSIN MADISON

Outline

- Introduction
- The Equilibrium and Magnetic Geometry
- Drift Models and Numerical Method
- Numerical Results
- Summary of Results

THE UNIVERSITY of WISCONSIN MADISON

HSX Stellarator

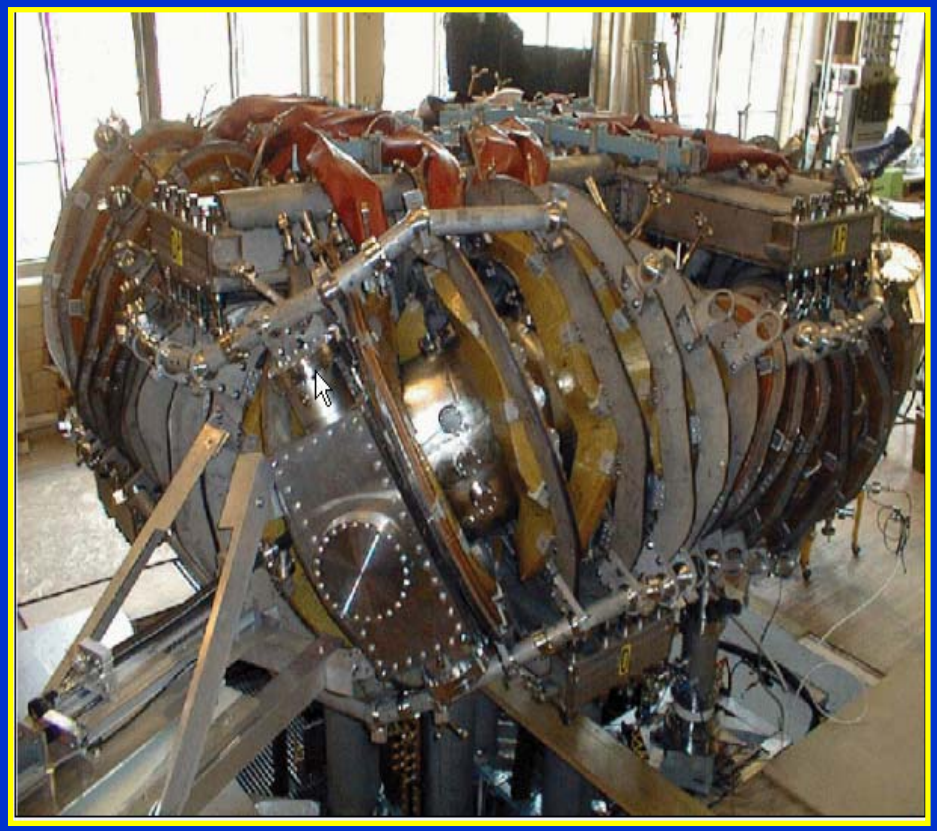

Engineering Hall, University of Wisconsin, Madison, USA

THE UNIVERSITY of WISCONSIN MADISON

Helically Symmetric Stellarator EXperiment (HSX)

- Helically axis of symmetry
- No toroidal curvature
- High effective transform, $|N-m\iota|=3$
- Small radial drift
- Small banana widths
- Small Pfirsch-Schluter currents
- Low neoclassical transport
- Good and bad curvature region rotates

$R = 1.2\,m$

$a = 0.12\,m$

$N = 4$

$i_a = 1.05$

$i_E = 1.12$

$AC = 48$

$\nu_e^* \leq 0.1$

$B_{\max} = 0.5T$

Symmetric can be broken

HSX is supportive to compact stellarators and has unique features

- Auxiliary coils provide flexibility for HSX

HSX can run in different modes of operation

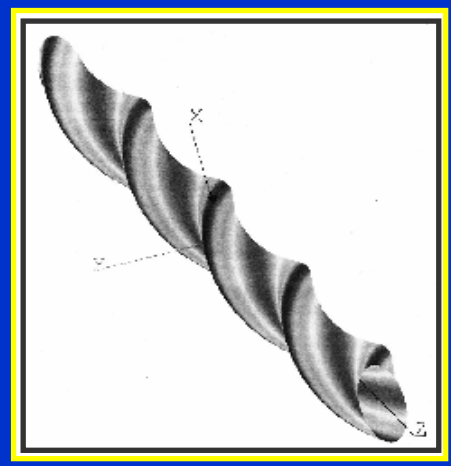

- **QHS (Quasi-helically Symmetric)**

→Current flows in main coil only

→Fully 3-D but symmetry in **|B|**

- **Mirror mode**

→ current flows in main and auxiliary coils

- **Anti Mirror mode**

→Current in auxiliary coils opposite to mirror case

Mirror and Anti mirror cases symmetry in **|B|** is broken

- The Equilibrium and Magnetic Geometry

The Equilibrium

- The VMEC code is used to generate equilibrium data for the nested magnetic surfaces.
- The Mapper code is used to transform VMEC data into Boozer coordinates.
- Equilibrium quantities are calculated on magnetic surfaces.

The Equilibrium

The cylindrical coordinates :

$$R=\sum_{m=0}^{n=n_p}\sum_{n=-n_t}^{n=n_t}R_{mn}(s)\cos(m\theta+nN\zeta)$$

$$\phi=\zeta-\frac{2\pi}{N}\sum_{m=0}^{n=n_p}\sum_{n=-n_t}^{n=n_t}\phi_{mn}(s)\sin(m\theta+nN\zeta)$$

$$z=\sum_{m=0}^{n=n_p}\sum_{n=-n_t}^{n=n_t}z_{mn}(s)\sin(m\theta+nN\zeta)$$

The position vector :

$$r_p=(R\cos\phi,R\sin\phi,z)$$

The covariant basis vectors :

$$e_s=\frac{\partial r_p}{\partial s},e_\theta=\frac{\partial r_p}{\partial\theta},e_\zeta=\frac{\partial r_p}{\partial\zeta}$$

The contravariant basis vectors :

$$\nabla s=\frac{e_\theta\times e_\zeta}{J},\nabla\theta=\frac{e_\zeta\times e_s}{J},\nabla\zeta=\frac{e_s\times e_\theta}{J}.$$

The Jacobean for Boozer coor.

$$J=e_s\cdot e_\theta\times e_\zeta=\frac{\psi^{\bullet}}{B^2}(B_\theta+qB_\zeta)$$

THE UNIVERSITY of WISCONSIN MADISON

The Magnetic Field

The magnetic field in Boozer coordinates:

$$\mathbf{B} = \nabla\alpha \times \nabla\psi = \psi^{\bullet} \nabla\alpha \times \nabla s,$$
$$\psi^{\bullet} \equiv \frac{d\psi}{ds} = \frac{B_0 \bar{a}^2}{2q}, \alpha = \zeta - q\theta, s = \frac{2\pi\psi}{\psi_p}$$

The field line curvature:

$$\kappa = \frac{\kappa_n}{\sqrt{g^{ss}}} \nabla s + \frac{\kappa_g}{\sqrt{g_{ss}}} \frac{\left(\psi^{\bullet} g^{ss}\right)}{B} \left(\nabla\alpha - \Lambda \nabla s\right)$$

The normal & geodesic components:

$$\kappa_n = \kappa \cdot \frac{\nabla s}{|\nabla s|}, \quad \kappa_g = \kappa \cdot \left(\frac{\nabla s}{|\nabla s|} \times e_{\|} \right).$$

The local magnetic shear:

$$s = -\left(\frac{\nabla s}{|\nabla s|} \times e_{\|} \right) \cdot \nabla \times \left(\frac{\nabla s}{|\nabla s|} \times e_{\|} \right) = \left(e_{\|} \cdot \nabla \right) \Lambda$$

Pressure and iota profiles

Pressure profile

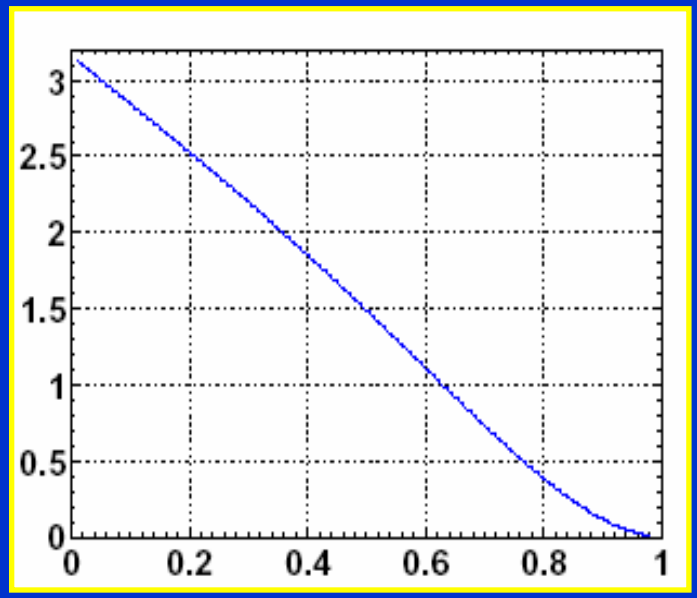

Rotational transform

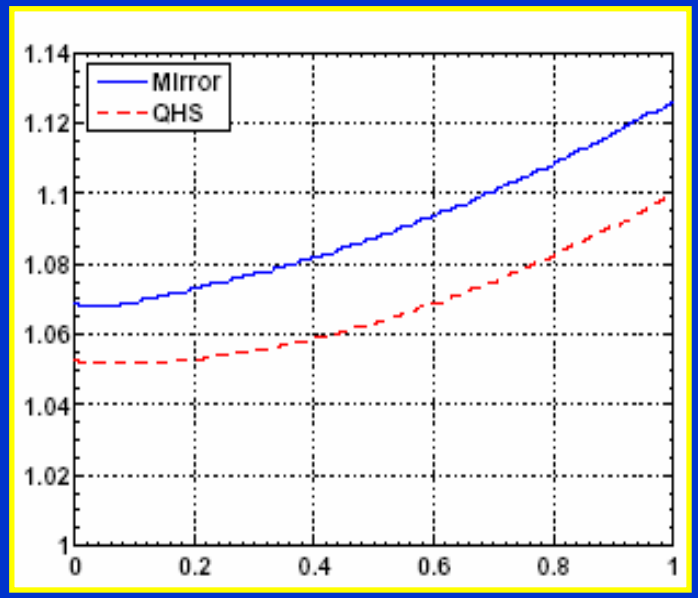

- **The transform for the QHS configuration is very similar to the Mirror**

Mirror is more elliptic

100*Magnetic well

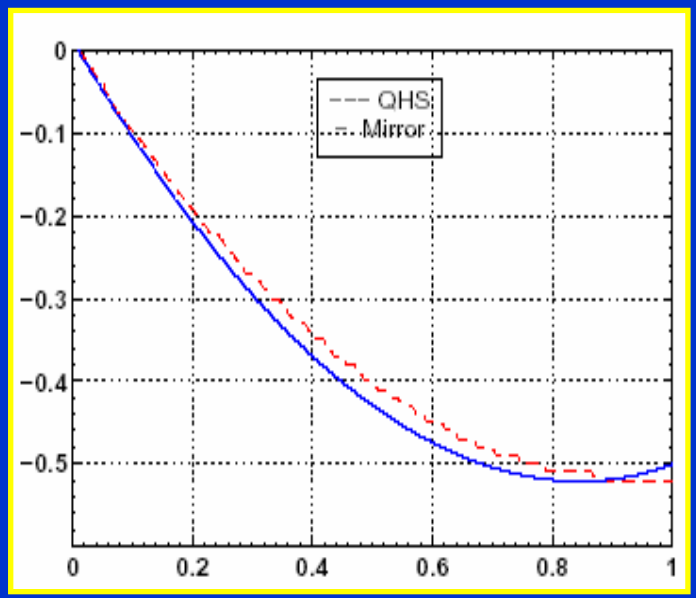

Ellipticity

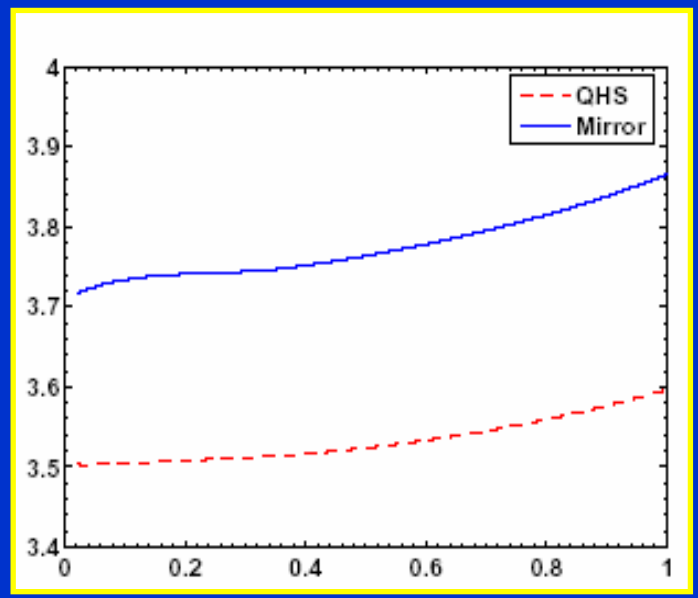

- **The stabilization is expected for an elongated equilibrium due to the reduction of magnetic drift frequency.**

THE UNIVERSITY of WISCONSIN MADISON

Flux surfaces are more compressed in Mirror

QHS

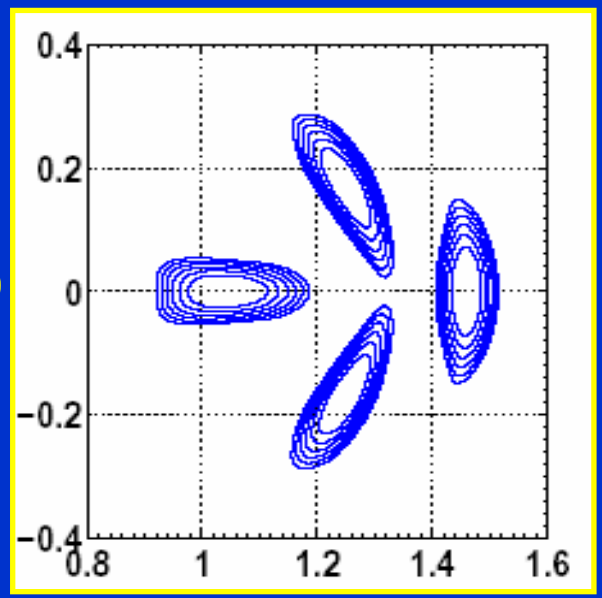

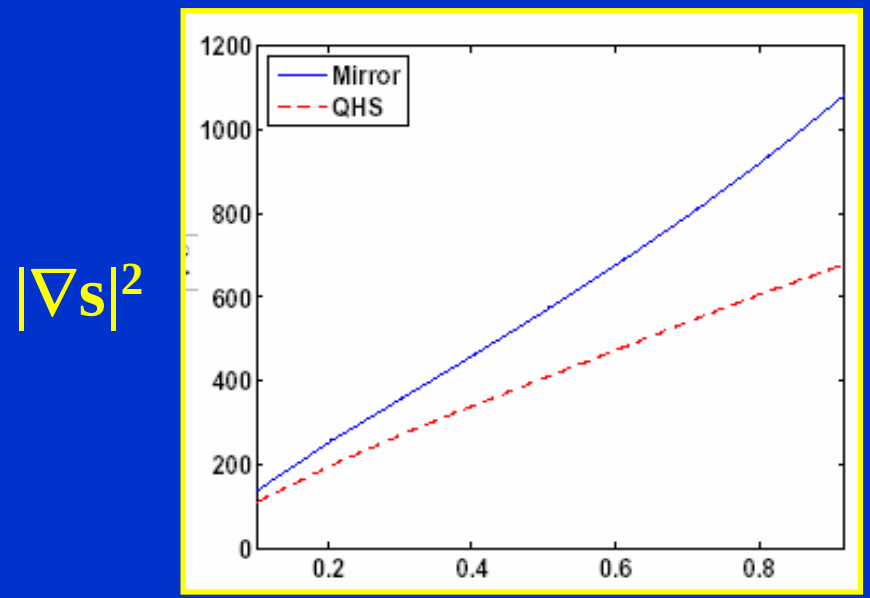

➢ **The flux surfaces are found more compressed in the Mirror case than the QHS configuration.**

Good and bad curvature region rotates

- At ζ_o=0, the good curvature region is on the inside of the surface.
- At ζ_o=1/4, the region of good curvature has moved to the bottom of the device.
- At ζ_o=1/2, the good curvature has moved to the outside of the device.
- At ζ_o=3/4, the good curvature has moved to the top of the flux surface.

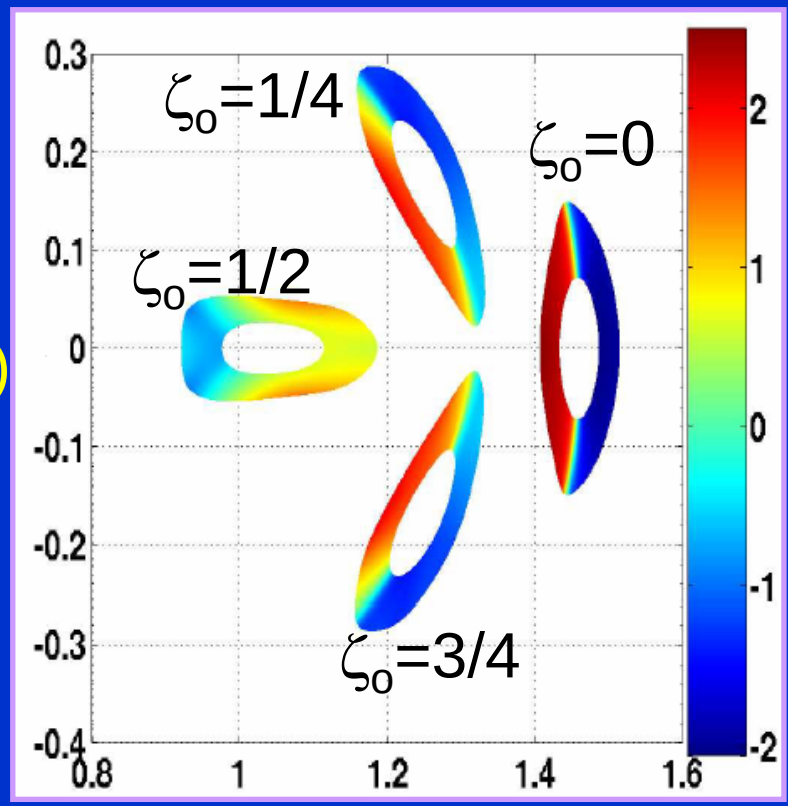

THE UNIVERSITY of WISCONSIN MADISON

Variation of |B| on the flux surface

QHS

Mirror

|B|

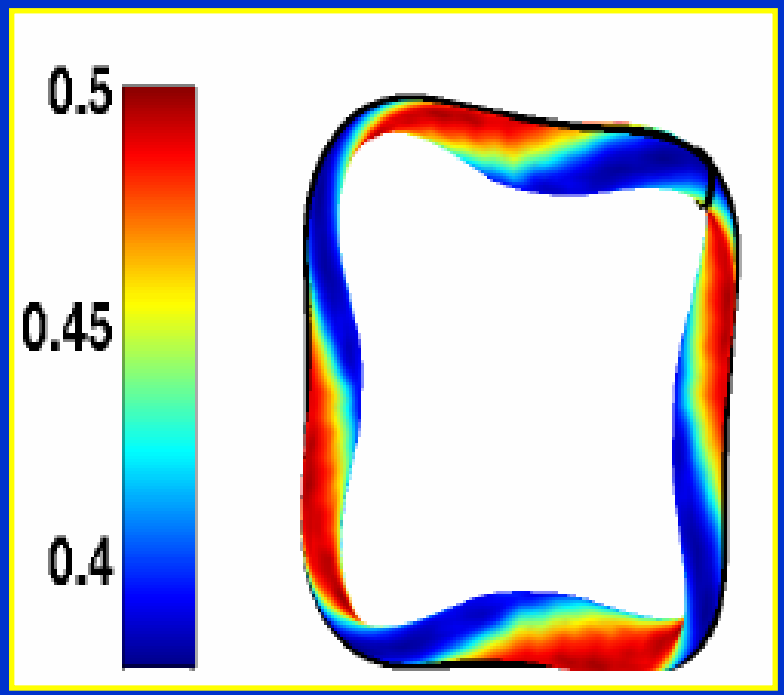

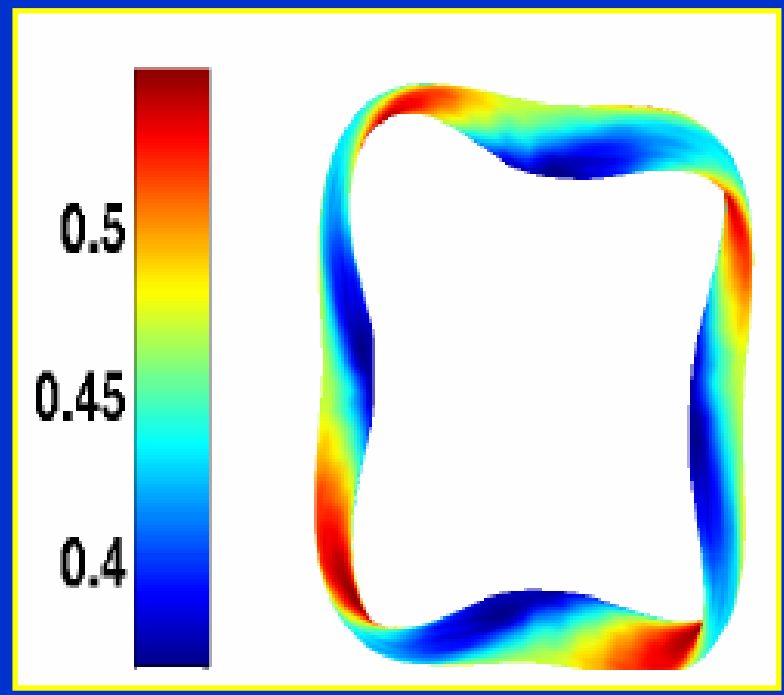

- The region of constant magnetic field illustrates the helical symmetry in the QHS configuration.

|B| along ζ

Mirror

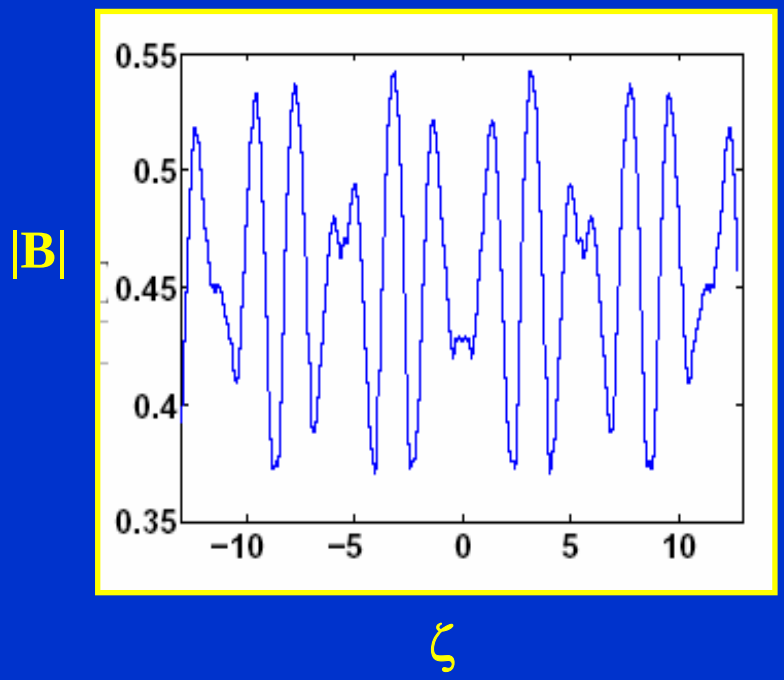

QHS

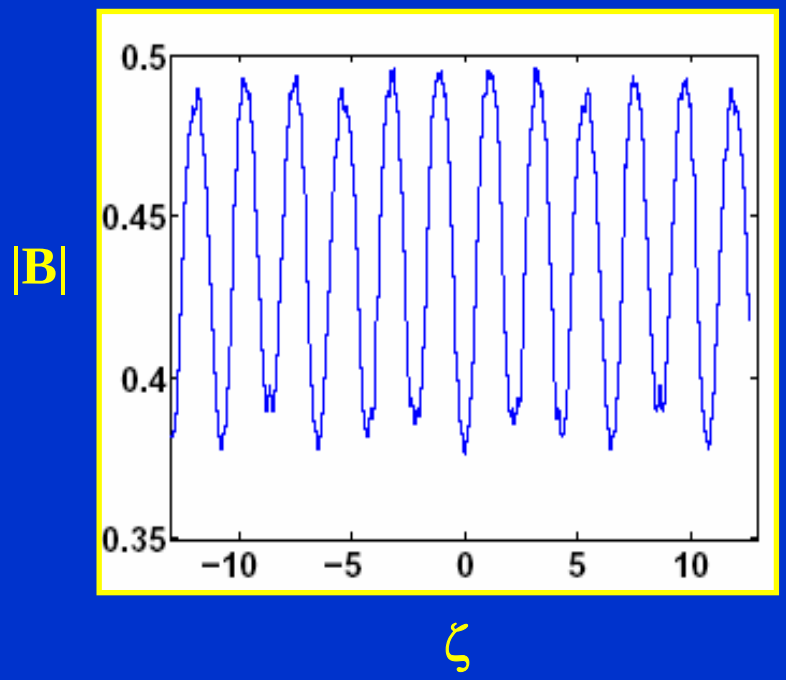

- The |B| strength minima and maxima for successive helical wells all have about the same value for the QHS case.

THE UNIVERSITY of WISCONSIN MADISON

Slightly more bad normal curvature in the QHS

Normal curvature

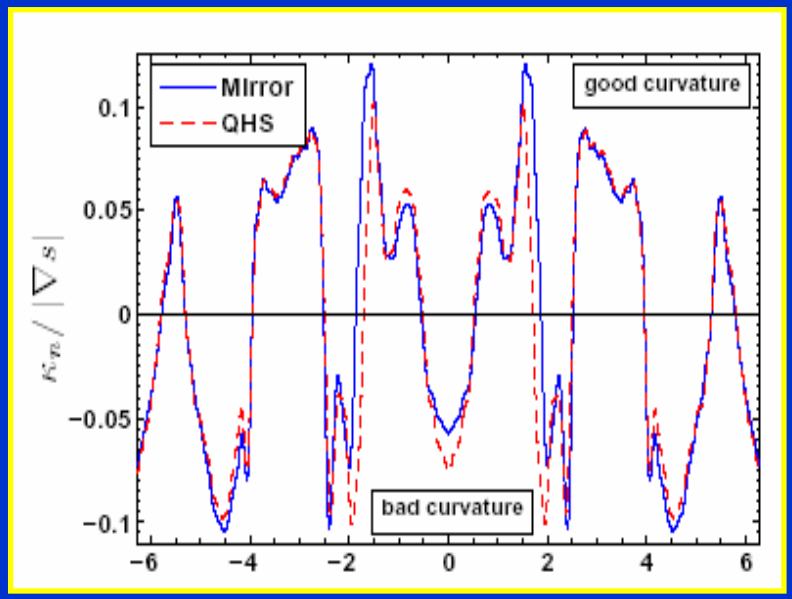

Geodesic curvature

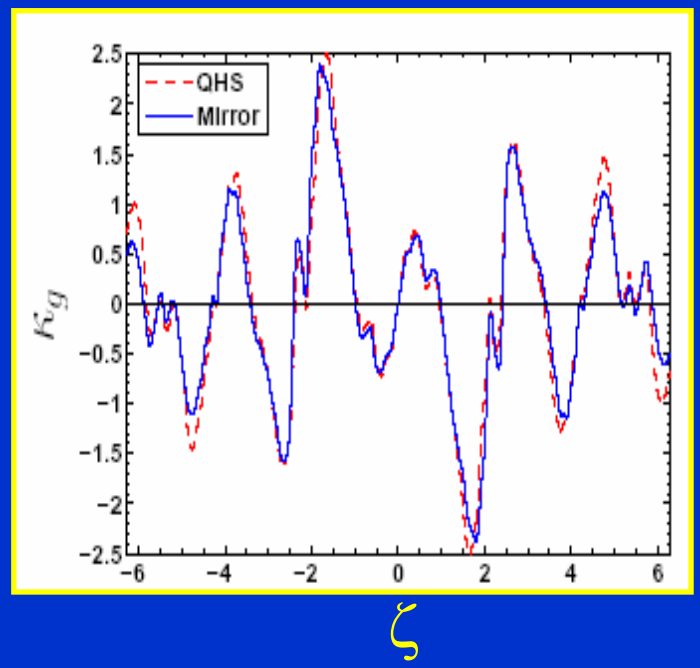

- Helical ripples which decreases the connection length between good and bad curvature is evident.
- Around ζ=0 slightly more bad normal curvature is found in the QHS case.

Local Magnetic shear and $k_\perp^2$

S

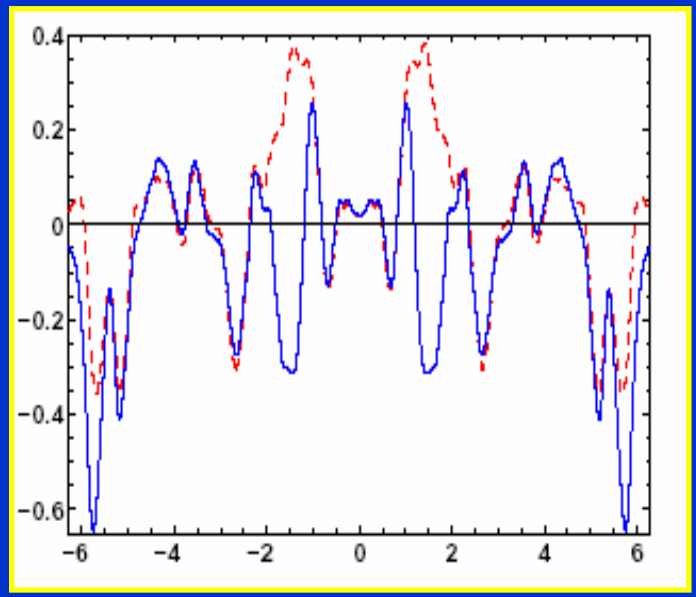

ζ

$k_\perp^2$

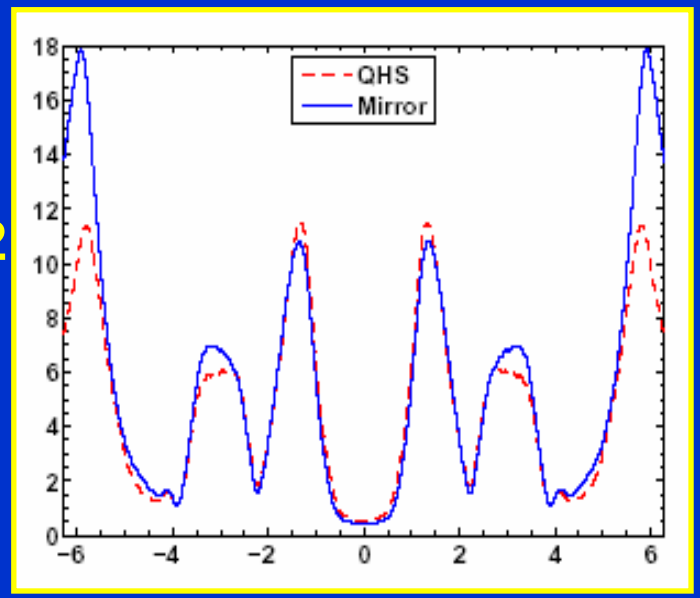

ζ

- More negative local magnetic shear region is found in the Mirror case.
- Most unstable modes occur where $\mathbf{k}_\perp^2$ is small (at ζ =0 for this equilibrium) and there is bad curvature there, so this is where the mode tends to localize.

- The electron drift wave model, numerical method and numerical results

THE UNIVERSITY of WISCONSIN MADISON

The i-delta model

The eigenvalue equation:

$$\left[\frac{c_s^2}{\omega^2}(e\|\bullet\nabla)^2 - \rho_i{}^2\nabla_\perp{}^2 - \left(\frac{1}{i\omega}\right)\mathrm{v}_*\bullet\nabla_\perp - \left(\frac{1}{i\omega}\right)\mathrm{v}_D\bullet\nabla_\perp + 1\right]\frac{e\phi}{T_e} = 0$$

Using ballooning mode formalism:

$$\frac{n_{e1}}{n_o} = (1 - \imath\delta)\frac{e\phi}{T_e}$$

$$\phi = \Phi(\zeta)\exp\left[-i\varepsilon^{-1}S(\psi,\alpha)\right]$$

$$\frac{d^2\phi}{d^2\zeta} - U\phi = 0$$

$$U = \left(\frac{JB}{\bullet}\right)^2\left[\chi\Omega(\Omega_* + \Omega_d) - \left(1 + \frac{B_o^2\chi_i^2\hat{k}_\perp^2}{B^2} + i\delta\right)\Omega^2\right]$$

Numerical Method

- The function U (ζ,Ω) on the domain [- ζ_{max}+ ζ_o, ζ_{max}+ ζ_o] for a given Ω

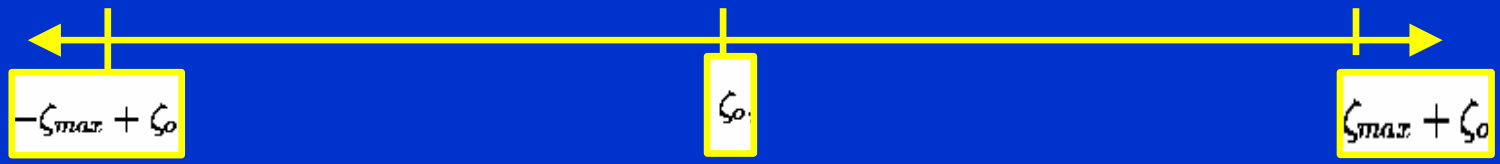

- The eigen function Φ at $\zeta = \pm \zeta_{max}$ and Φ' are calculated by using sixth order Numerov scheme

- The eigen frequency is determined which satisfies the condition:

$$f(\Omega) = \frac{\Phi'_+}{\Phi_+} - \frac{\Phi'_-}{\Phi_-} = 0$$

on a complex frequency plane.

Similar Drift modes using i-delta model

QHS

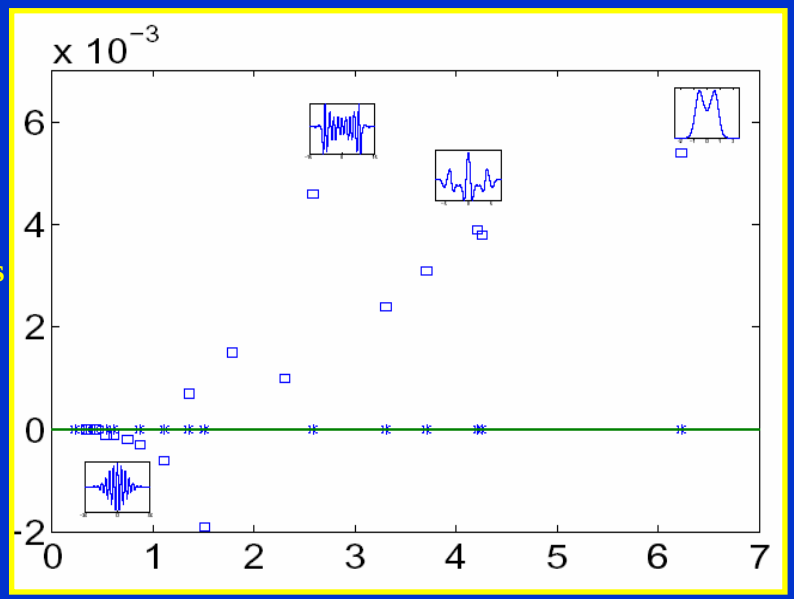

$\gamma R/C_s$

$R\omega/C_s$

Mirror

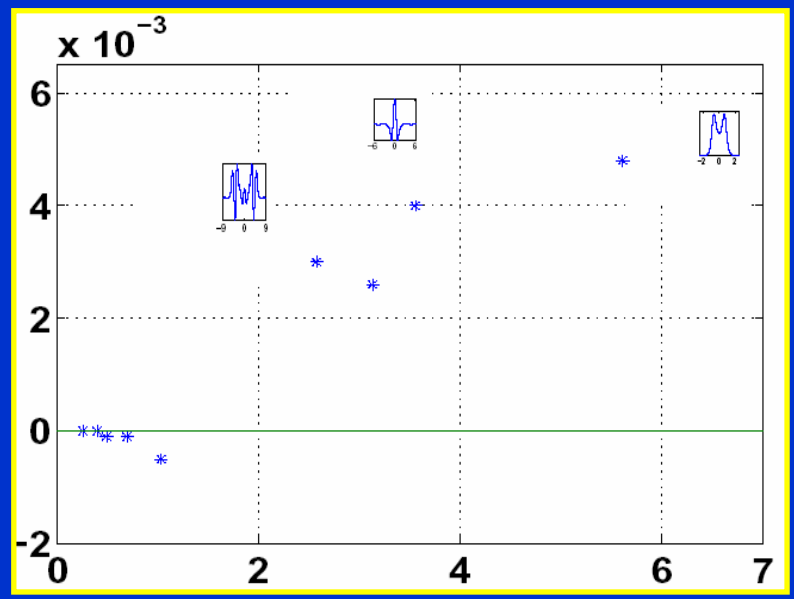

$R\omega/C_s$

- At low frequencies modes are extended along the field line and for higher frequencies they are more localized.

THE UNIVERSITY of WISCONSIN MADISON

Slightly more unstable in QHS

Effective potential

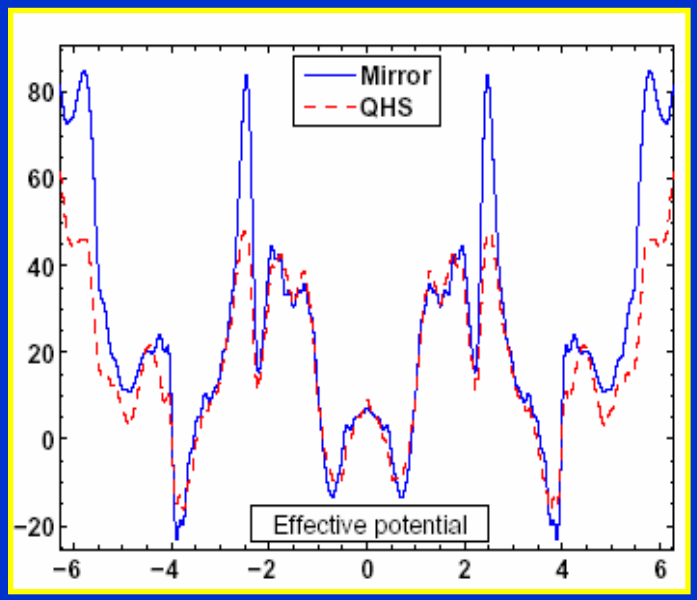

Eigenfunction

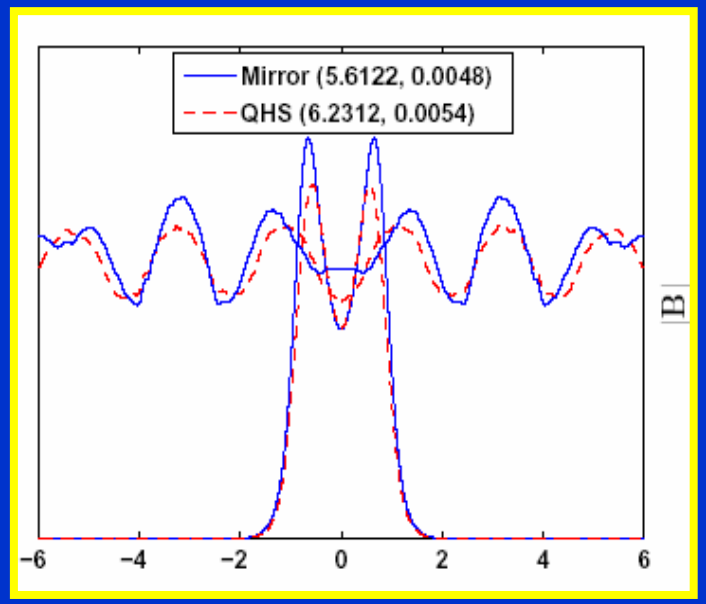

- **The modes are localized in the first couple of helical peaks of the potential.**

Variation of the growth rate in one field period of the QHS

|B|

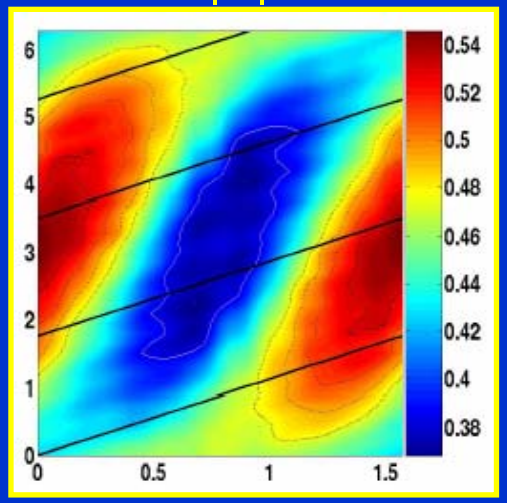

Growth rate

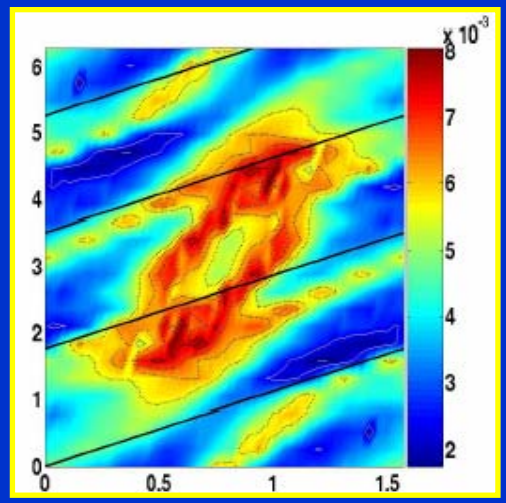

Geodesic curvature

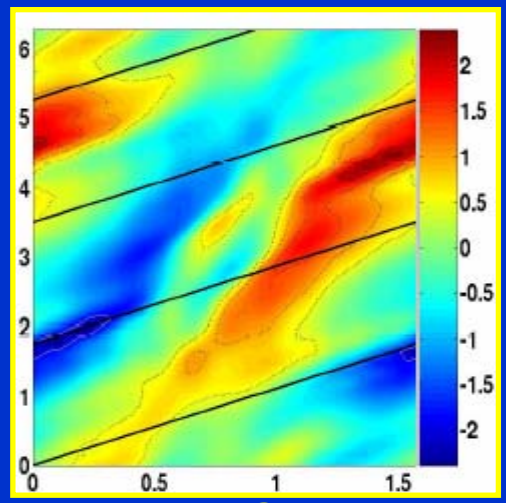

Normal curvature

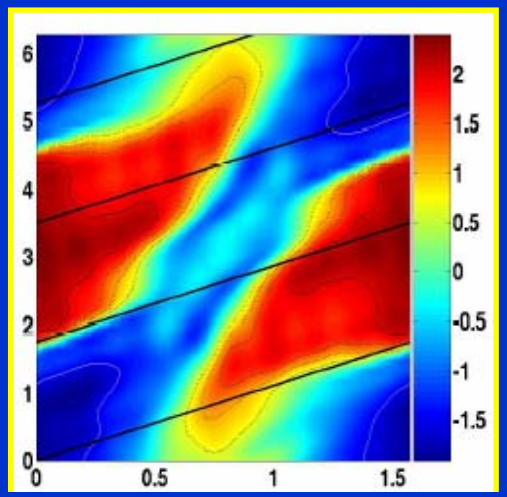

Local magnetic shear

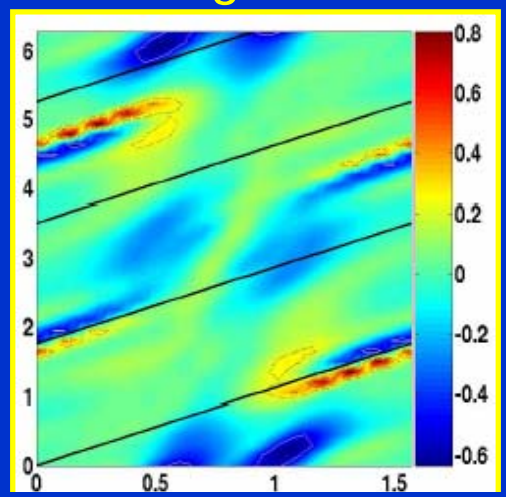

$|\nabla s|^2$

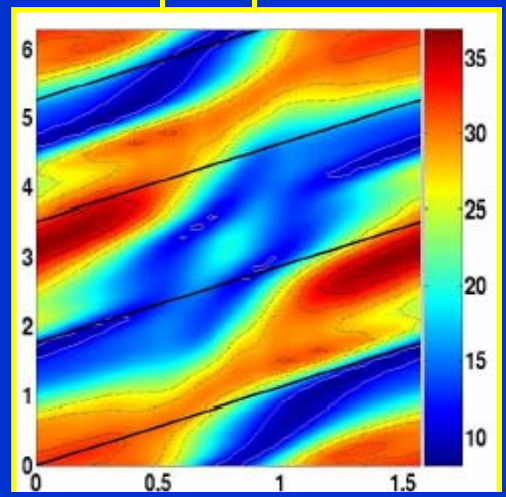

- The highest growth rate is found in regions where normal curvature is bad, local magnetic shear and geodesic curvature is small and |B| is minimum

- The ITG Model and Results

The ITG model

The drift wave equation in a low beta plasma :

$$\frac{d^2\psi}{d^2\zeta} - \left(\frac{2\chi_i JB}{\bar{a}q\varepsilon_n \bar{R}\dot{\psi}}\right)^2 \left[\left(H^{-1} - \frac{\bar{a}\varepsilon_n \Omega_d}{2}\right)\Omega - \left\{H^{-1} + \left(\frac{\chi_i B_o}{B}\right)^2 \left(\hat{k}_\perp \bullet \hat{k}_\perp\right)\Omega^2\right\}\right]\psi = 0$$

We introduce the transformation: $\psi = H\,\phi$ where:

and:

$$H = 1 + \frac{1}{\tau} + \tau^{-1}\left[\frac{\left(2/3\right)\Omega + \left(\eta_i - \left(2/3\right)\right)}{\Omega + \left(5/6\tau\right)\bar{a}\varepsilon_n \Omega_d}\right]$$

The ITG model(contd.)

$$\Omega = \frac{\omega}{\omega_{*e}}, \varepsilon_n = \frac{L_n}{R}, \chi_i = (\varepsilon \bar{a})^{-1} q \rho_i \left(\frac{\partial S}{\partial \alpha} \right),$$

$$\hat{k}_\perp = \hat{k}_\perp (s, \alpha, \zeta; \theta_k) = \frac{\bar{a}}{q} \left[\nabla \zeta - q \nabla \theta - \left(\frac{\zeta - \zeta_o}{q} - \theta_k \right) \frac{dq}{ds} \nabla s \right],$$

$$\Omega_d = \Omega_d (s, \alpha, \zeta) = \frac{B_o \bar{R} \left[\mathbf{B} \times (\kappa + \nabla \ln B) \right]}{B^2} \bullet \hat{k}_\perp,$$

$$\nabla \ln B = \frac{1}{2} \left[\left(\frac{d}{ds} \ln (B_\theta + q B_\zeta) - \frac{\partial \ln J}{\partial s} \right) \nabla s - \frac{\partial \ln J}{\partial \theta} \nabla \theta - \frac{\partial \ln J}{\partial \zeta} \nabla \zeta \right]$$

$$L_n^{-1} = - \frac{d \ln n_o}{ds} \hat{s} \bullet \nabla s \Big|_{\zeta = 0}, \quad \text{where} \quad \hat{s} \equiv \frac{\nabla s}{|\nabla s|}.$$

$$b = (k_\perp \rho_i)^2 = \chi_i^2 (\hat{k}_\perp \bullet \hat{k}_\perp) = \left(\varepsilon^{-1} \frac{\partial S}{\partial \alpha} \right)^2 |\nabla \alpha \bullet \nabla \alpha|_{\zeta = 0}.$$

ITG modes are similar in the QHS and Mirror

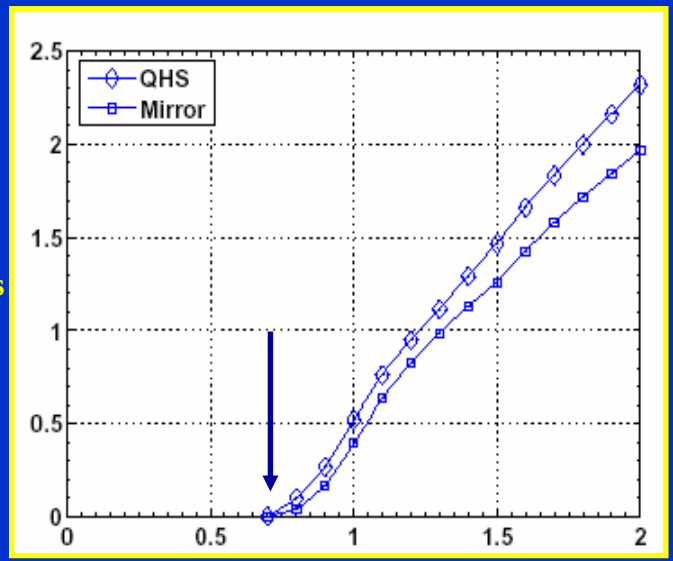

$\gamma R/C_s$

η_i

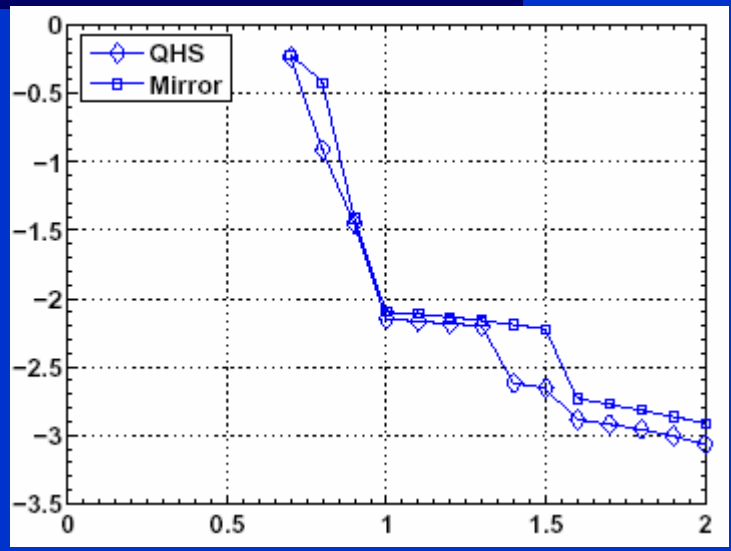

$\omega R/C_s$

η_i

s=0.8980, b=0.1, θ_k =0.0, $\in_n$ =0.1 & τ=1.0

- **The threshold for instability in terms of η_i is approximately 2/3**

Positive local shear in the bad curvature region is found to be destabilizing

$\gamma R/C_s$

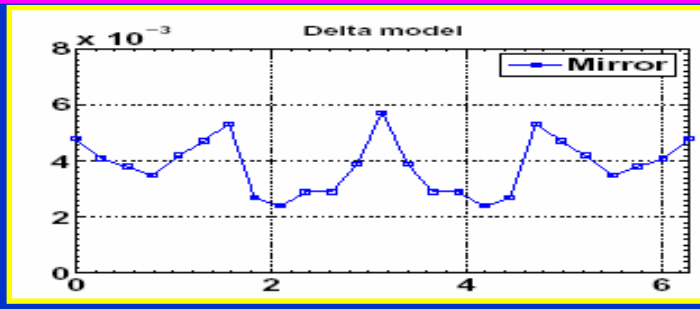

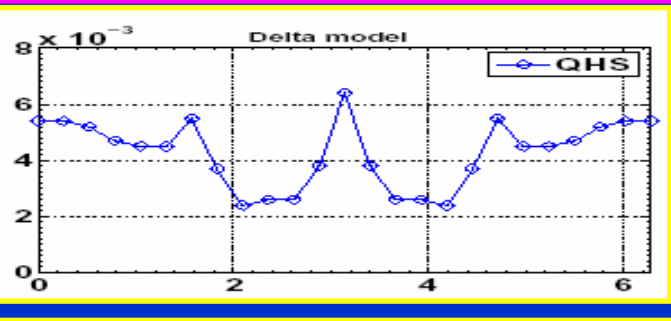

$\gamma R/C_s$

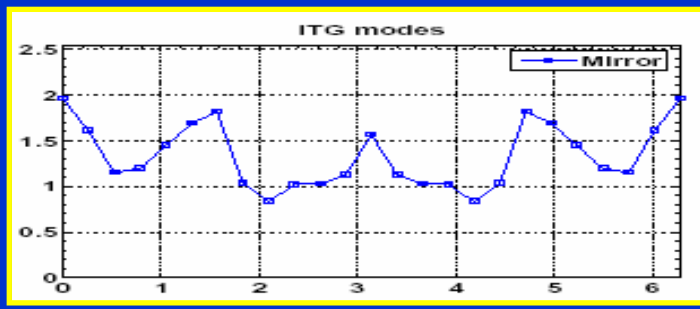

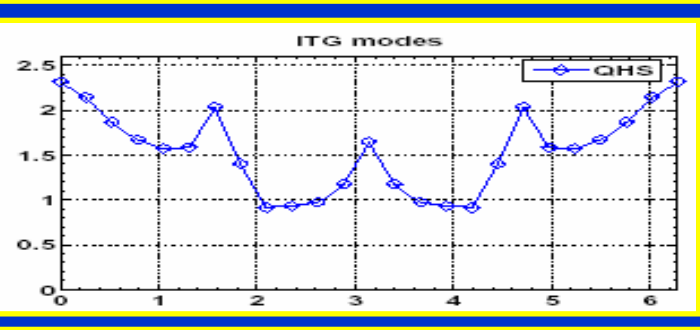

S

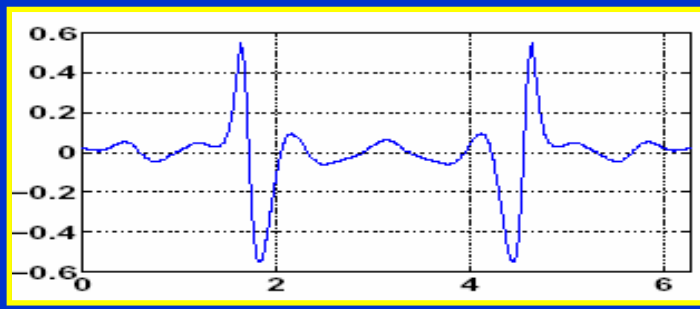

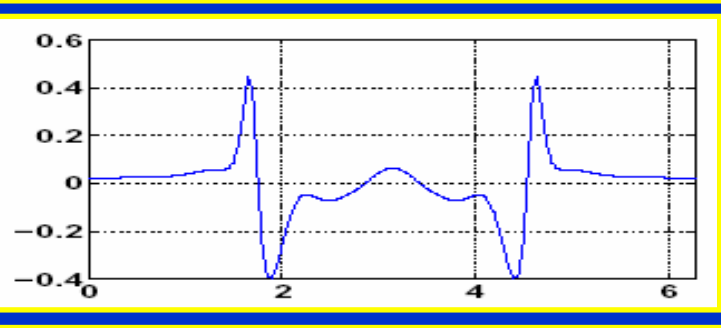

$\kappa_n, \kappa_g, |B|$

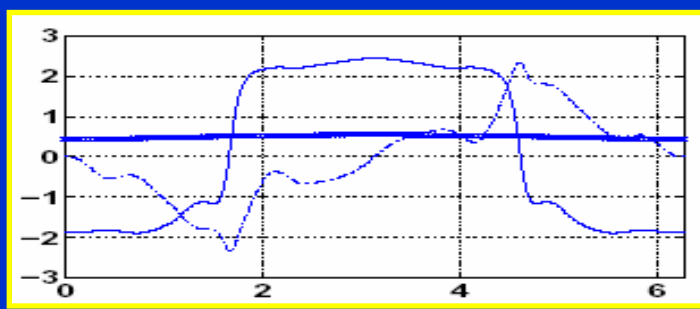

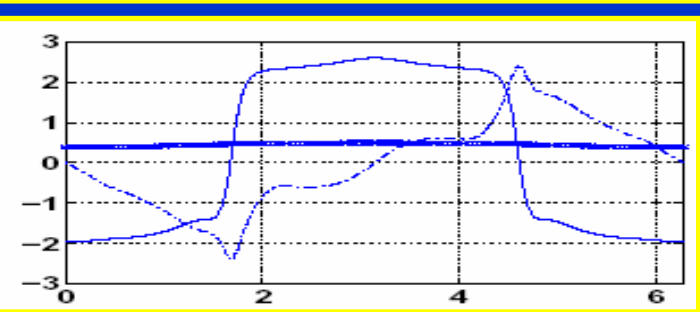

- Modes are found to be more dependent on the local shear in the iδ model whereas, in the ITG model the role of normal curvature is found dominant.

THE UNIVERSITY of WISCONSIN MADISON

ITG Modes

$$\Omega_d = -2\chi \frac{\bar{R}}{\bar{a}} \left\{ \frac{\kappa_n}{\sqrt{g^{ss}}} - \frac{\kappa_g}{\sqrt{g^{ss}}} \frac{B_o}{B} \chi_g (\Lambda + \theta_k \hat{q}) \right\}$$

$b \equiv k^2_\perp \rho_s^2 = 0.1$, $\theta_k = 0.0$, $\epsilon_n \equiv L_n/R = 0.2$, $\eta_i \; (\equiv L_n/L_{ti}) = 3$, $\tau = 1.0$ & $s = 0.7$

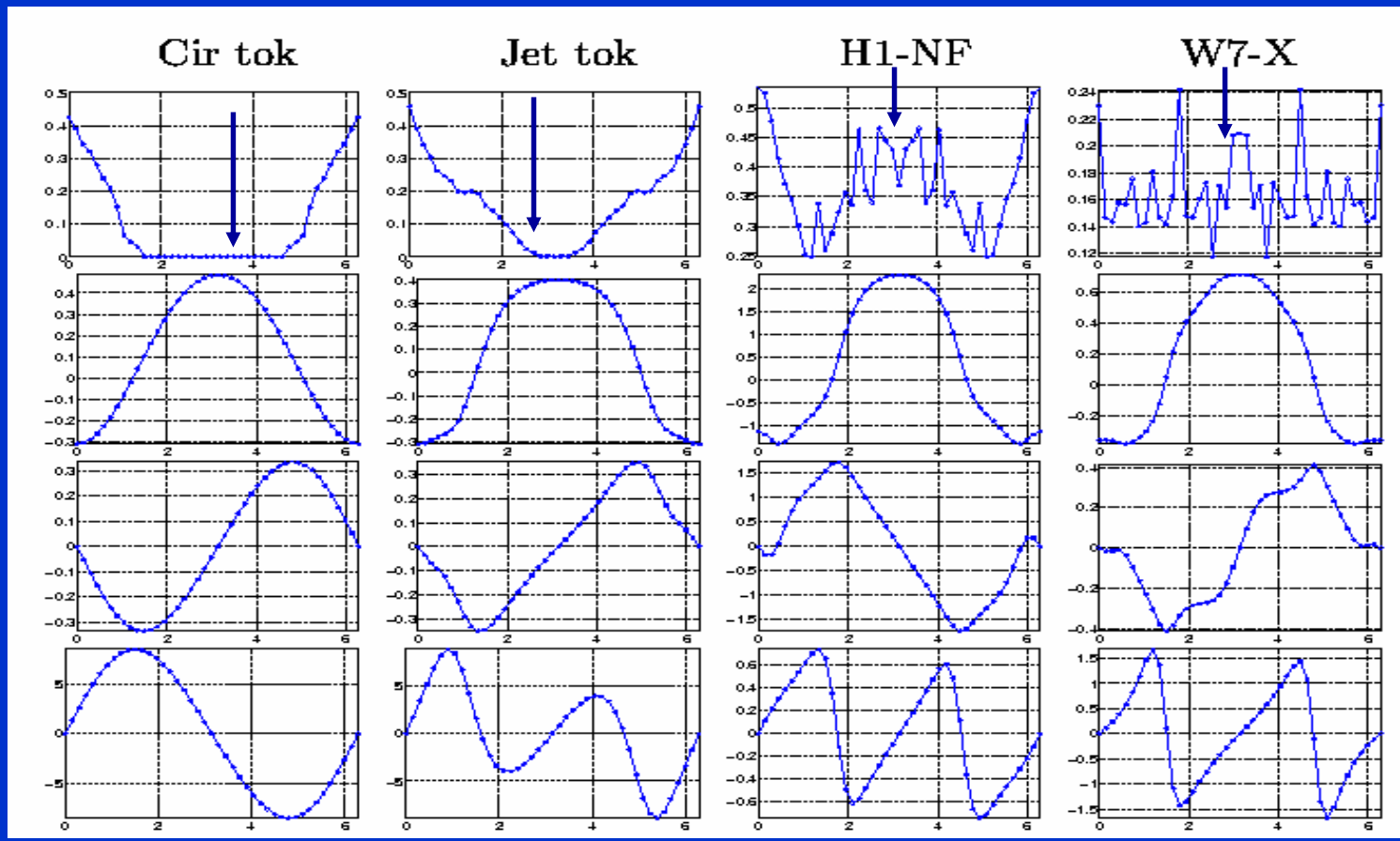

- Dissipative trapped electron modes

THE UNIVERSITY of WISCONSIN MADISON

DTEM Introduction

- Trapped electron modes are basically drift waves that are destabilized by a population of trapped electron
- The basic mechanism for instability of DTEM is the detrapping of electron population by collisions with ions
- The trapped particles effects will play an important role in the limit $\upsilon_{ef}\tau_b << 1$
- The connection length of the helical field ripples in stellarators ($L_c=R/|N-m\iota|$) is shorter than toridal magnetic well in tokamaks ($L_c \sim qR$)

Dissipative Trapped electron model

The perturbed electron distribution function :

$$f_{e1} = \frac{|e|\phi f_{e0}}{T_e} + g_e$$

where

$$\left(-i\omega + \upsilon_{ef} + i\omega_{de} + iv_{\|}\hat{e}\bullet\nabla\right)g_e = \left(1 - \frac{\omega_{*e}\left\{1+\eta_e\left(E/T_e+1.5\right)\right\}}{\omega}\right)\frac{i|e|\omega\phi}{T_e} f_{e0}$$

The effective collision frequency can be written as:

$$\upsilon_{ef} = \frac{\upsilon\left(v = v_e\right)}{\varepsilon}\left(\frac{v_e}{v}\right)^3$$

$$\omega_b \sim |\, v_{\|}\hat{e}\bullet\nabla \,| > \omega, \omega_{*e}, \upsilon_{ef}, \omega_{de}$$

Dissipative Trapped electron model

Then to lowest order equation reduces to :

$$(v_{\parallel}\hat{e}\bullet\nabla)g_e$$

To next order:

$$g_e=\frac{i|e|f_{e0}}{T_e}\left(\frac{\omega-\omega_{*e}\{1+\eta_e(E/T_e+1.5)\}}{\upsilon_{ef}}\right)\langle\phi\rangle,\ \text{where}\ \langle\phi\rangle=\frac{\int dt_b\phi}{\int dt_b}$$

The total perturbed electron density:

$$\frac{\delta n_e}{n_e}=\frac{e}{T_e}\left(\phi-i\frac{2}{\sqrt{\pi}\upsilon_{ef}}(\omega_{*e}-\omega+1.5\eta_e\omega_{*e})\int\frac{Bd\Lambda}{\Lambda^{\frac{3}{2}}\sqrt{\Lambda-B}}\langle\phi\rangle\right)$$

The above response is obtained by changing variables

$$v_{\perp}=\sqrt{\frac{2BE}{m\Lambda}}\ \text{to}\ E,\ v_{\parallel}=\sqrt{\frac{2E}{m}\left(1-\frac{B}{\Lambda}\right)}\ \text{to}\ \Lambda=\frac{E}{\mu}$$

Dissipative Trapped electron model

Ion density response

The ion density perturbation :

$$\left(\frac{c_s^2}{\omega^2}(e\|\bullet\nabla)^2-\rho i^2\nabla_\perp^2-\left(\frac{1}{i\omega}\right)v_*\bullet\nabla_\perp-\left(\frac{1}{i\omega}\right)v_D\bullet\nabla_\perp\right)\frac{e\phi}{T_e}+\frac{\delta n i}{n i}=0$$

The electron response:

$$\frac{\delta n_e}{n_e}=\frac{e}{T_e}\left(\phi-i\frac{2}{\sqrt{\pi}\upsilon_{ef}}(\omega_{*e}-\omega+1.5\eta_e\omega_{*e})\int\frac{Bd\Lambda}{\Lambda^{\frac{3}{2}}\sqrt{\Lambda-B}}\langle\phi\rangle\right)$$

The perturbation theory:

$$\delta\omega=\frac{\int d\zeta/B^2\Phi^*R\Phi}{\int d\zeta/B^2\Phi^*(dL/d\omega)\Phi}$$

Dissipative Trapped electron model

A change in frequency due to non adiabatic electron contribution :

$$\frac{\delta\omega}{\omega_0} = i\frac{4}{\upsilon_{ef}\sqrt{\pi}}\left(\left(\omega_{*e} - \omega_0 + 1.5\eta_e\omega_{*e}\right)\frac{H_1}{H_2}\right)$$

$$H_1 = \sum \int_{B\,\min}^{B\,\max} \frac{d\Lambda}{\Lambda^{\frac{3}{2}}} \frac{\left|\int_{\varsigma_-}^{\varsigma_+} d\varsigma \Phi_0 / B\sqrt{\Lambda - B}\right|^2}{\int_{\varsigma_-}^{\varsigma_+} d\varsigma / B\sqrt{\Lambda - B}}$$

and

$$H_2 = \int_0^\infty \frac{d\varsigma}{B^2}\left|\Phi_0\right|^2 \frac{B_0}{B}\left(2k_\perp^2\rho^2\chi^2 - \chi\frac{\omega_{*e} + \omega_d}{\omega_0} + 2\right)$$

THE UNIVERSITY of WISCONSIN MADISON

Most unstable modes are found different in QHS and Mirror configurations

Mirror

QHS

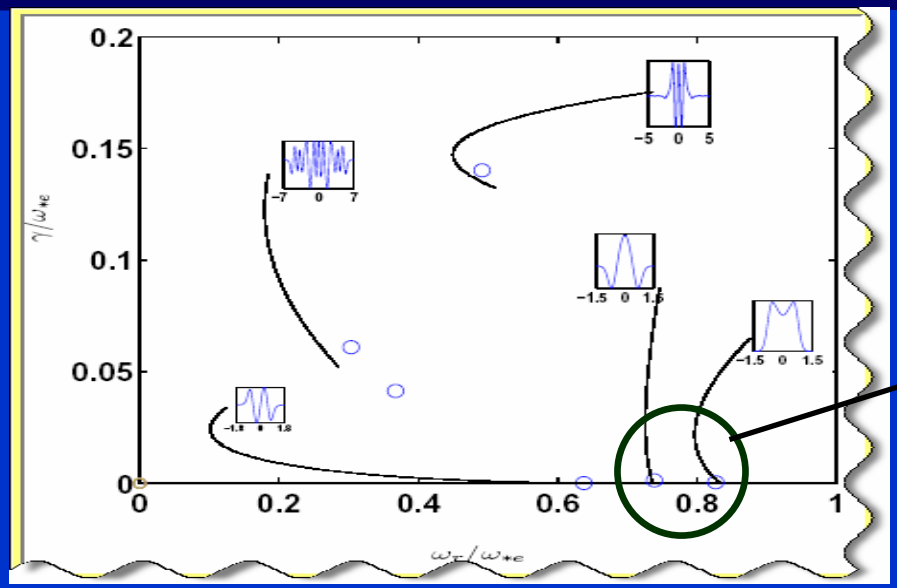

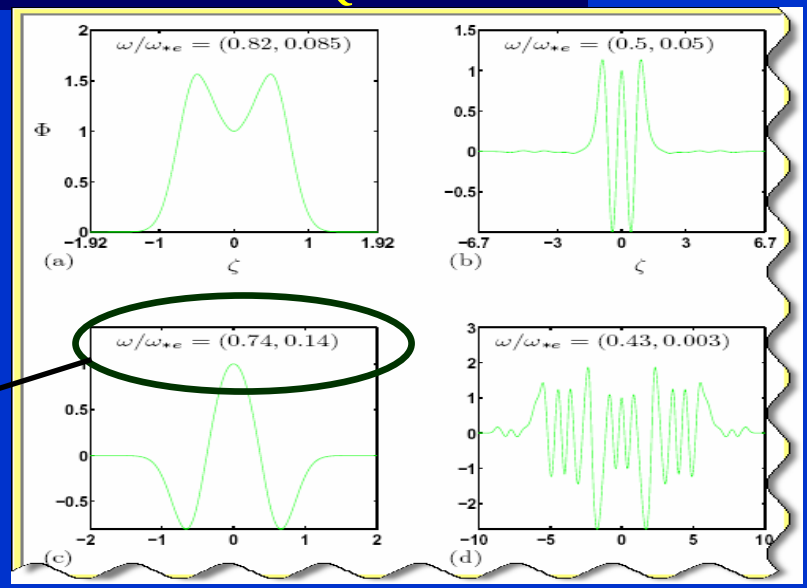

- Most localized (helical) modes are found to be marginally stabilized in the mirror geometry
- The most unstable modes in the Mirror case is found to be more extended (toroidal modes). They are excited due to dominance of toroidal wells in the |B| structure.

THE UNIVERSITY of WISCONSIN MADISON

Growthrate increases for peak density profiles

QHS configuration

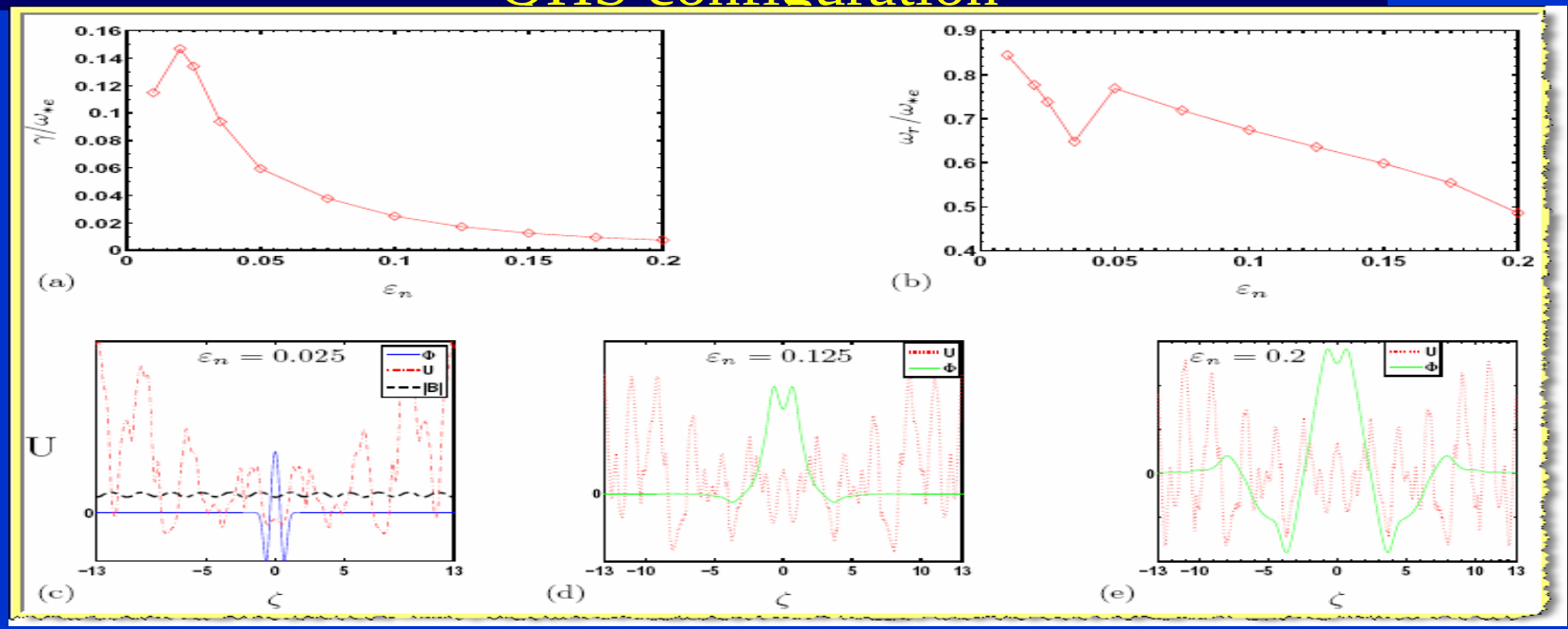

- The max. growth rate corresponds to the mode which is localized to the smallest number of helical wells and has the steep density profile.
- As the density profile is broadened the structure of the effective potential changes, eigenfunction becomes extended, with a corresponding decrease in growth rate and real frequency

THE UNIVERSITY of WISCONSIN MADISON

Growthrate decreases for peak density profiles

Mirror configuration

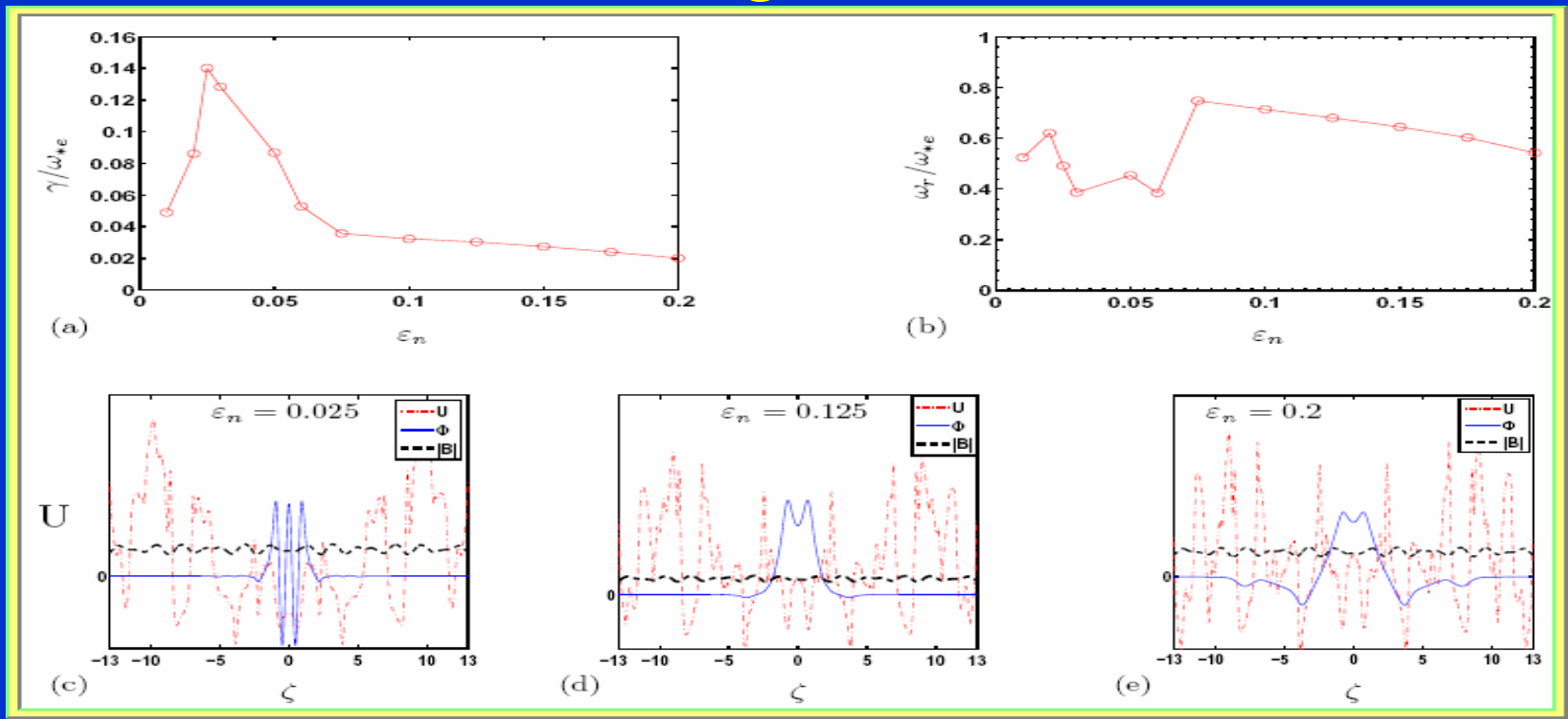

➢ **The largest growth rate corresponds to the mode which is localized in the toroidal wells of |B|**

THE UNIVERSITY of WISCONSIN MADISON

The maximum growth rate for different density profiles occurs at the same mode number

QHS configuration

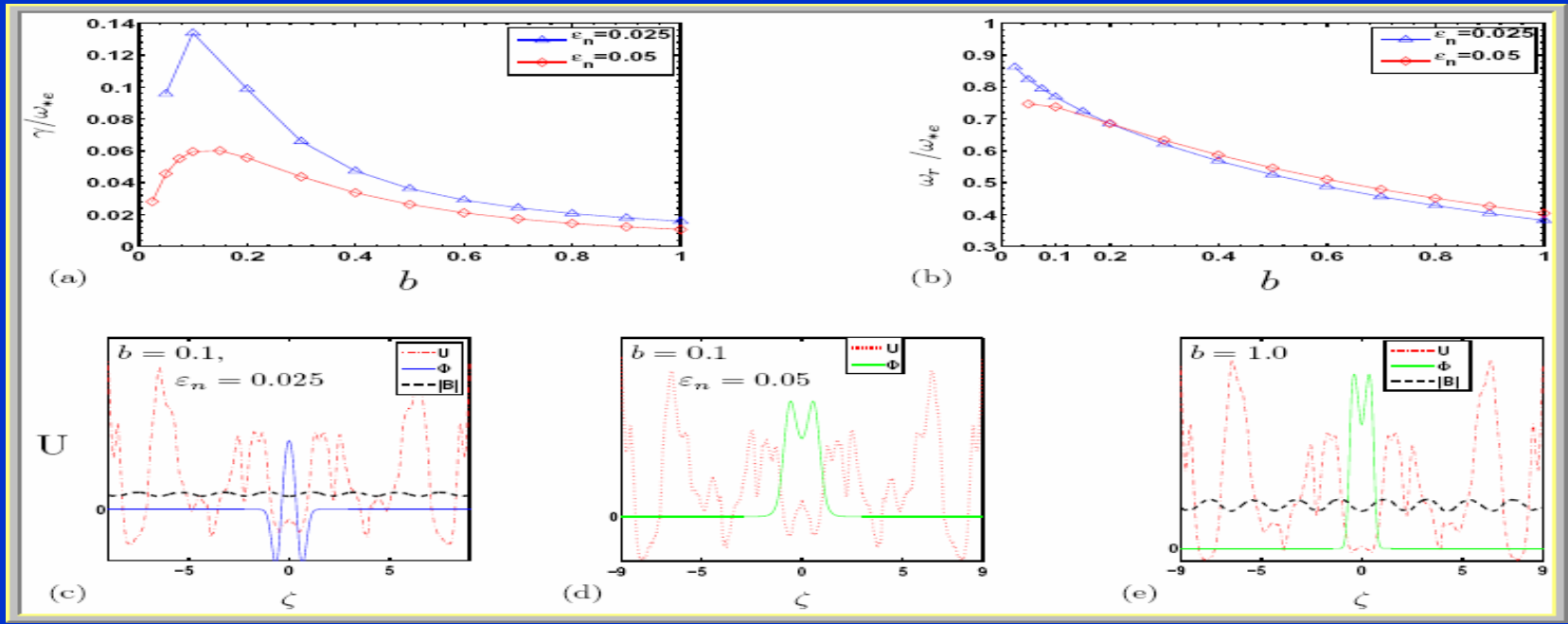

- A *b* increases, eigenfunctions become more and more localized and trapped in the first helical well of |B| and effective potential.

- The growth rate of DTEM decreases with the increase of *b*>0.1.

THE UNIVERSITY of WISCONSIN MADISON

Modes become completely stable at $b \geq 0.4$

Mirror configuration

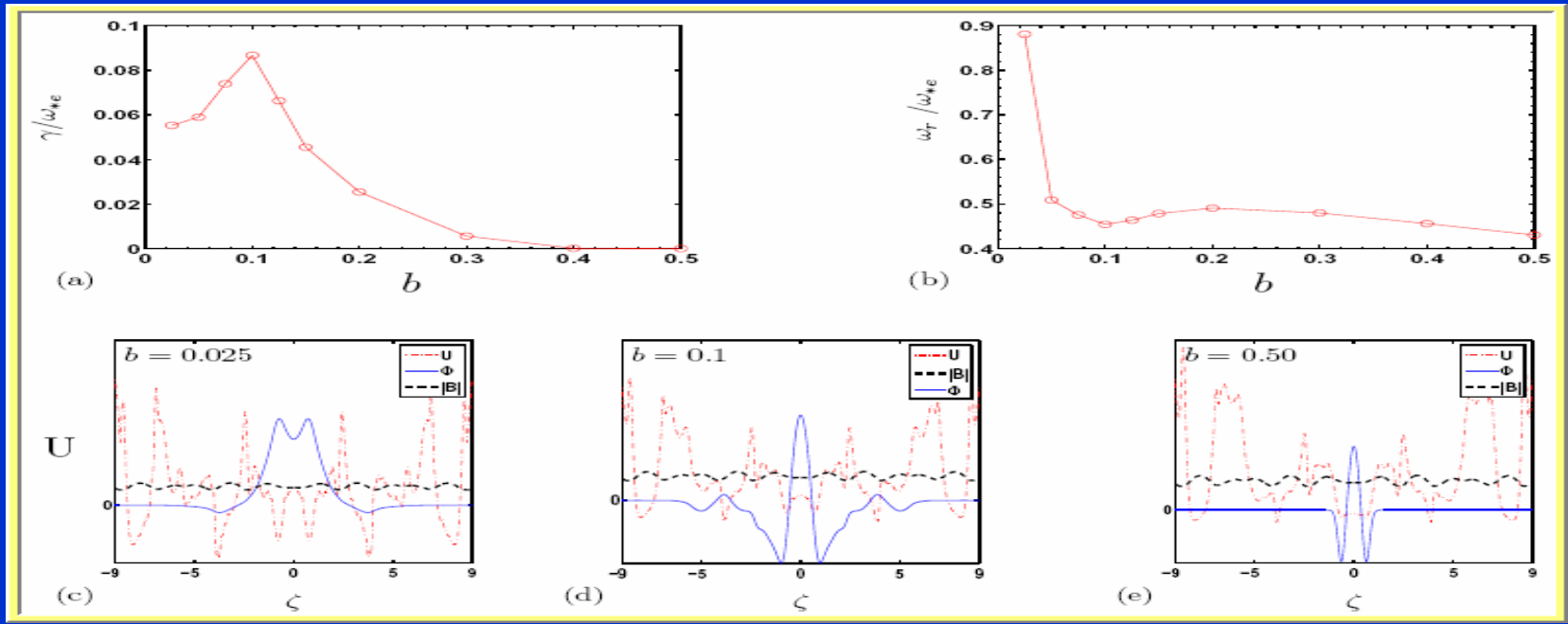

- Modes become completely stable at b=0.4 due to the FLR effects and due to the shallow helical ripples at ζ =0. This is not a case for the QHS configuration.

Localized modes have less growthrate in Mirror configuration

QHS and Mirror configuration

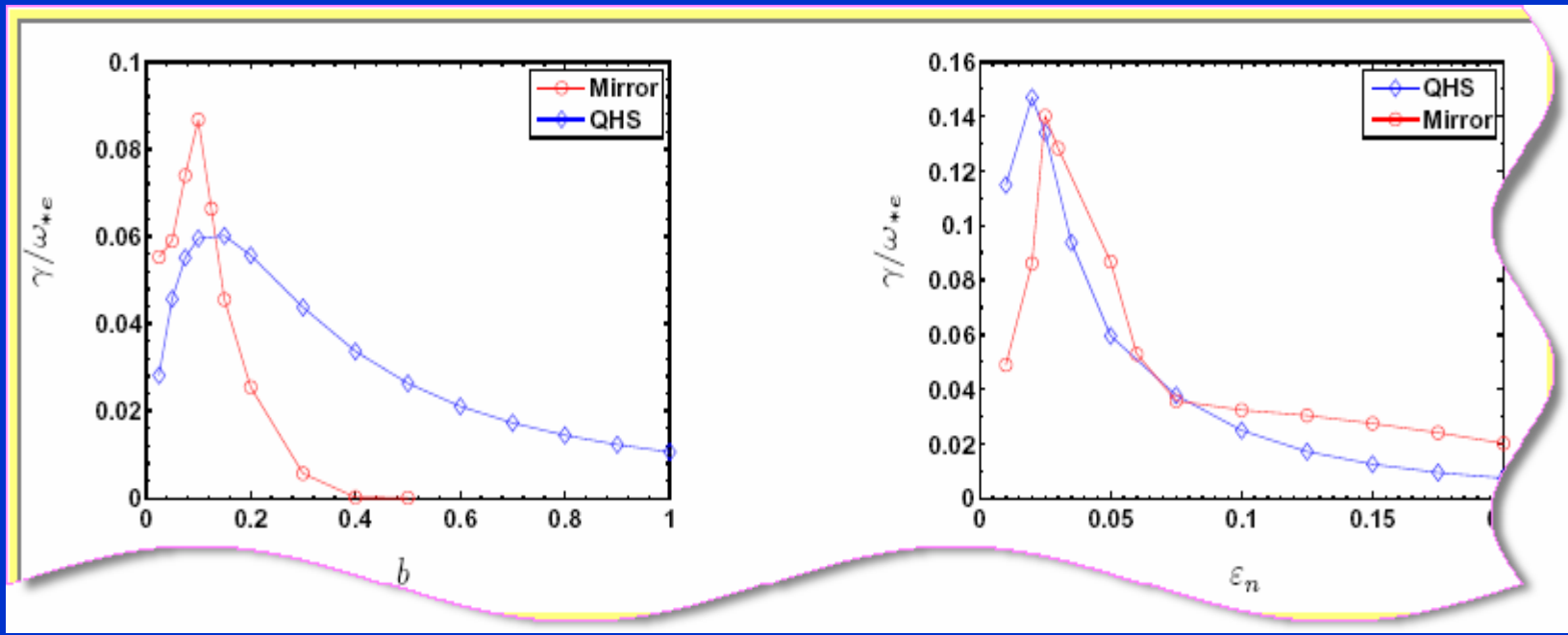

➢**The magnitude of the growth rate is found to be higher in the Mirror configuration except for cases with peaked density profile and for *b*>0.15 (localized modes).**

THE UNIVERSITY of WISCONSIN MADISON

Plasma is marginally stable to the DTEM in the core

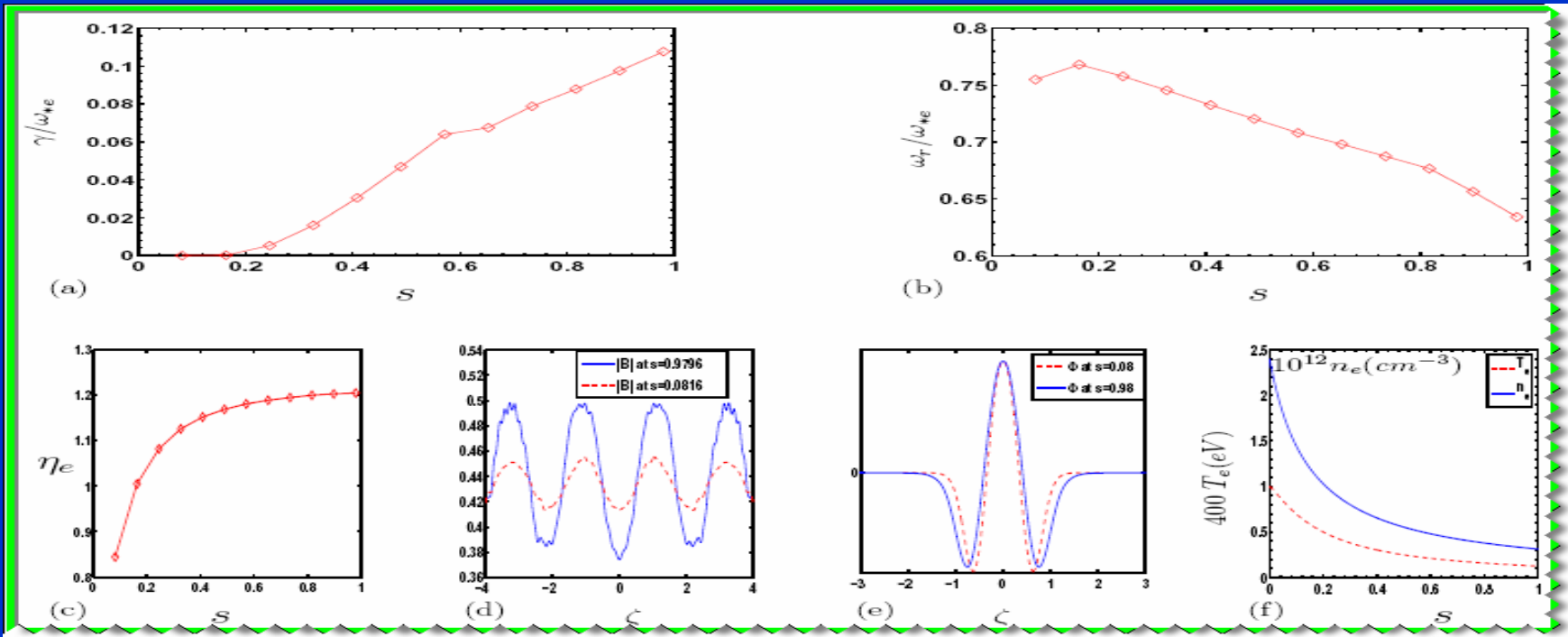

➢The stability of the core region is due to the structure of |B|, which has shallow helical wells and therefore does not helically localize eigenfunctions.

THE UNIVERSITY of WISCONSIN MADISON

DTEM is stable in the region of good curvature

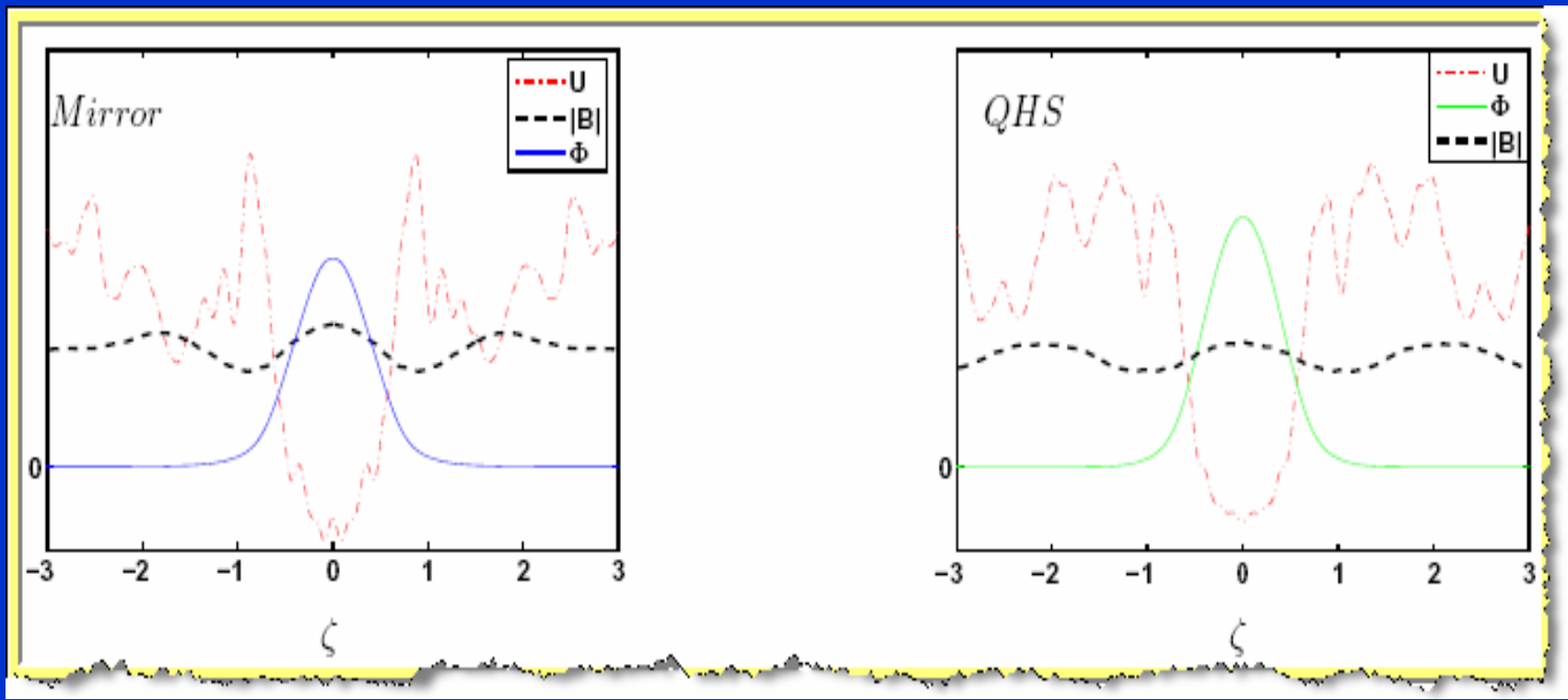

- Localized modes are found to be stabilized in the region of good curvature and in the anti helical well of |B| in both geometries.

Summary of Results

- **Equilibria:** The local magnetic shear and the geodesic curvature vanish in both configuration where the normal curvature is most destabilizing
- **Curvature effects:** The most unstable modes are found in the region where normal curvature is bad; they are found less affected by geodesic curvature
- **Local magnetic shear effects:** The field lines, which cross the region of negative values of local magnetic shear have the most stable eigenmode. However, the large positive local magnetic shear is found to be destabilizing in the bad curvature region.
- **ITG modes:** The threshold stability in terms of η_i is found around 2/3.
- **DTEM:** The helically trapped modes are found to be most destabilizing in the QHS configuration, while in the Mirror configuration the toroidally trapped modes are found unstable. The magnitude of the growth rate is found to be higher in the Mirror configuration except for cases with peaked density profile. The edge is found to be more unstable as compared to center.


THE UNIVERSITY of WISCONSIN MADISON
Thank You!